Halogen-Substituted 2,6-Bis(imino)pyridyl Iron and Cobalt Complexes: Highly Active Catalysts for Polymerization and Oligomerization of Ethylene

Yaofeng Chen,† Ruifang Chen,† Changtao Qian,*,† Xicheng Dong,‡ and Jie Sun†

State Key Laboratory of Organometallic Chemistry, and Laboratory of Computer Chemistry, Shanghai Institute of Organic Chemistry, Chinese Academy of Sciences, 354 Fenglin Road, Shanghai 200032, China

Received April 22, 2003

A series of halogen-substituted 2,6-bis(imino)pyridyl ligands and their iron and cobalt complexes [{2,6-(2,6-$X^1X^2C_6H_3N{=}CCH_3)_2C_5H_3N$}$MCl_2$] ($X^1 = X^2 =$ Br, M = Fe (**1**), Co (**2**); $X^1 = X^2 =$ Cl, M = Fe (**3**), Co (**4**); $X^1 =$ Cl, $X^2 =$ H, M = Fe (**5**), Co (**6**); $X^1 =$ Br, $X^2 =$ H, M = Fe (**7**), Co (**8**); $X^1 =$ I, $X^2 =$ H, M = Fe (**9**), Co (**10**)) and [M{2,6-(2,6-$X^1X^2C_6H_3N{=}CCH_3)_2C_5H_3N$}$_2$]$^{2+}$-[$MCl_4$]$^{2-}$ ($X^1 =$ F, $X^2 =$ H, M = Fe (**11**)) have been synthesized. The molecular structures of complexes **1**, **8**, **9**, **10**, and **11** were determined by X-ray diffraction. Crystallographic analyses indicate that **1**, **8**, **9**, and **10** are five-coordinate complexes, while **11** is an ion-pair complex with one six-coordinate iron center and one four-coordinate iron center. These metal coordinative complexes, activated by modified methylaluminoxane (MMAO), lead to highly active ethylene polymerization and/or oligomerization catalysts. The catalyst productivity and product properties crucially depended on the metal center and the halogen substituents on the aryl rings. The catalyst productivities are in the range of (0−73.0) × 10^6 g/mol of cat·h. The species **11**, having ion-pair structure, is inactive. In particular, the product molar masses were changed from high molar mass (M_w of 377 000) to low molar mass oligomers by varying the halogen substituents. NMR and thermal analyses reveal the polymer is highly linear. The oligomer products follow a Schulz−Flory distribution with high selectivity for linear α-olefins. The effects of reaction condition on the polymerization and oligomerization have also been studied.

1. Introduction

Polyethylene (PE) is a very important industrial plastic material, with more than 100 billion pounds of polyethylene produced every year.[1] Among them, the production of high-density polyethylene (HDPE) prepared using catalytic ethylene polymerization contributes over 40 billion pounds. Linear α-olefins are versatile chemical intermediates for a wide range of industrial and consumer products. The major use of linear α-olefins is polyethylene comonomer, surfactants, and lubricants. Oligomerization of ethylene is currently the primary resource of linear α-olefins. Since Ziegler's original work in $TiCl_4/AlR_3$-catalyzed ethylene polymerization and AlR_3-catalyzed ethylene oligomerization, many catalysts for ethylene polymerization[2−11] and oligomerization[12−18] have been synthesized. Due to the huge commerical value of HDPE and linear α-olefins, exploring new ethylene polymerization and oligomerization catalysts aimed at controlling the product properties and reducing the product cost is still of topical interest. Recently, a new class of iron and cobalt complexes bearing bis(imino) pyridyl ligands was reported by Brookhart[19−21] and Gibson.[22] These iron and

* Corresponding author. E-mail: qianct@mail.sioc.ac.cn. Fax: 0086-21-64166128.
† State Key Laboratory of Organometallic Chemistry.
‡ Laboratory of Computer Chemistry.

(1) Ittel, S. D.; Johnson, L. K.; Brookhart, M. *Chem. Rev.* **2000**, *100*, 1169.
(2) Jordan, R. F. *Adv. Organomet. Chem.* **1991**, *32*, 325.
(3) Kaminsky, W.; Arndt, M. *Adv. Polym. Sci.* **1997**, *127*, 144.
(4) Jeske, G.; Lauke, H.; Mauermann, H.; Swepstone, P. N.; Schumann, H.; Marks, T. J. *J. Am. Chem. Soc.* **1985**, *107*, 8091.
(5) Van der Linder, A.; Schaverien, C. J.; Meijboom, N.; Ganter, C.; Orpen, G. A. *J. Am. Chem. Soc.* **1995**, *117*, 3008.
(6) Scollard, J. D.; McConville, D. H.; Payne, N. C.; Vittal, J. J. *Macromolecules* **1996**, *29*, 5241.
(7) Baumann, R.; Davis, W. M.; Schrock, R. B. *J. Am. Chem. Soc.* **1997**, *119*, 3830.
(8) Younkin, T. R.; Connor, E. F.; Henderson, J. I.; Friedrich, S. K.; Grubbs, R. H.; Bansleben, D. A. *Science* **2000**, *287*, 460.
(9) Johnson, L. K.; Killian, C. M.; Brookhart, M. *J. Am. Chem. Soc.* **1995**, *117*, 6414.
(10) Britovsek, G. P. J.; Gibson, V. C.; Wass, D. F. *Angew. Chem., Int. Ed.* **1999**, *38*, 428.
(11) Matsui, S.; Mitani, M.; Saito, J.; Tohi, Y.; Makio, H.; Matsukawa, N.; Takagi, Y.; Tsuru, K.; Nitabaru, M.; Nakano, T.; Tanaka, H.; Kashiwa, N.; Fujita, T. *J. Am. Chem. Soc.* **2001**, *123*, 6847.
(12) Keim, W. *Angew. Chem., Int. Ed. Engl.* **1990**, *29*, 235.
(13) Cavell, K. J. *Aust. J. Chem.* **1994**, *47*, 769.
(14) Killian, C. M.; Johnson, L. K.; Brookhart, M. *Organometallics* **1997**, *16*, 2005.
(15) Komon, Z. J. A.; Bu, X.; Bazan, G. C. *J. Am. Chem. Soc.* **2000**, *122*, 12379.
(16) Byrikhina, N. A.; Pechatnikos, E. L. *J. Appl. Chem.* **1986**, *59*, 332.
(17) Briggs, J. R. *Chem. Commun.* **1989**, 674.
(18) Vogt, D. In *Applied Homogeneous Catalysis with Organometallic Compounds*, Vol. 1; Cornils, B., Herrmann, W. A., Eds.; VCH: New York, 1996; p 245.
(19) Small, B. L.; Brookhart, M. *Polym. Prepr. (Am. Chem. Soc., Div. Polym. Chem.)* **1998**, *39*, 213.
(20) Small, B. L.; Brookhart, M.; Bennett, A. M. A. *J. Am. Chem. Soc.* **1998**, *120*, 4049.
(21) Small, B. L.; Brookhart, M. *J. Am. Chem. Soc.* **1998**, *120*, 7143.

10.1021/om0302894 CCC: $25.00
Publication on Web 09/11/2003

Scheme 1

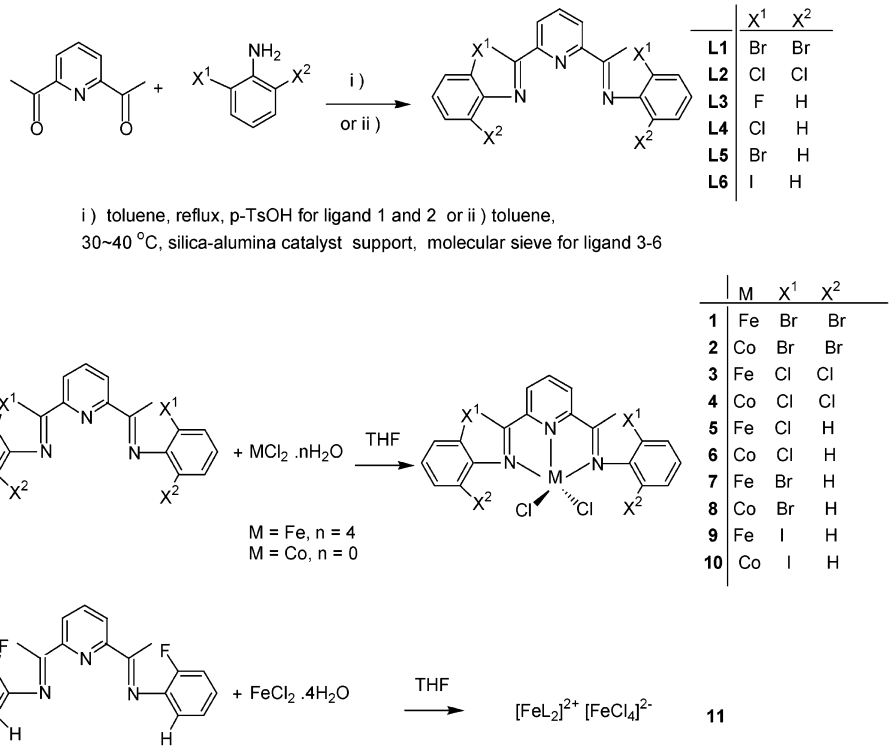

cobalt complexes exhibit high activities in ethylene polymerization and oligomerization. The product is strictly linear polymer with high density. The oligomers consist of ≥95% linear α-olefins. The product molar mass is dependent on the size of alkyl substituents at the *ortho* postion of imine aryl rings and ranges from high molar mass to low molar mass oligomers.

Halogens are a family of interesting substituents. The electronegativities decrease from fluorine to iodine with the values of 4.0, 3.0, 2.8, and 2.5, respectively, while the covalent radius (Å) increases in the same order: 0.72, 0.99, 1.14, and 1.33, respectively.[23] The halogen substituents lead to not only steric effects but also electronic effects. Compared to the small difference in electronic effect originating from changing the alkyl groups, the electronic effect from varying halogens is much more significant due to the large difference in their electronegativities. The halogens are generally electron-attracting, while the alkyls are electron-donating. Our previous results showed that difluoro-substituted 2,6-bis(imino)pyridyl iron complexes were very highly active catalysts for ethylene oligomerization.[24] Employing different halogens as the substituents on the imine aryl rings in the catalysts and studying the relationship between catalyst productivity, product properties and halogen subsituents are expected to be of interest. Nevertheless, to the best of our knowledge, no such work has been published.[25] Recently, we synthesized a series of halogen-substituted 2,6-bis(imino)-pyridyl ligands and their iron and cobalt complexes. The investigation of their catalytic activities in ethylene polymerization and oligomerization using MMAO as cocatalyst has shown that these iron and cobalt complexes are very active for ethylene polymerization and oligomerization, and the product molar masses are closely dependent on the different halogen atoms as substituents. Herein, we report our research results.

2. Results and Discussion

2.1. Synthesis and Characterization of Ligands and Corresponding Metal Complexes. The 2,6-bis(imino)pyridyl ligands with alkyl substituents at the *ortho* position of aryl groups can be readily prepared by condensation of the appropriate aniline with 2,6-diacetylpyridine using formic acid (or glacial acetic acid) as catalyst.[20,21,26] However, these conditions are not optimal for the preparation of 2,6-bis(imino)pyridyl ligands with halogen substituents. The ligands **L1** and **L2** were synthesized by the reaction of diketone with the corresponding halogenated aniline in the presence of a catalytic amount of *p*-toluene sulfonic acid in toluene with removal of water by azeotropic distillation (Scheme 1). Ligands **L3**−**L6** were synthesized in satisfactory yield (56−75%) in the presence of a catalytic amount of silica−alumina catalyst support with molecular sieves as the water adsorbent. This technique also offers the advantages of mild reaction conditions and use of much less solvent.[27] Ligands **L1**−**L6** were char-

(22) Britovsek, G. P. J.; Gibson, V. C.; Kimberley, B. S.; Maddox, P. J.; McTavish, S. J.; Solan, G. A.; White, A. J. P.; Williams, D. J. *Chem. Commun.* **1998**, 849.

(23) Linus Pauling. *The Nature of The Chemical Bond*, 3rd ed.; Carnell University Press: Ithaca, NY, 1973.

(24) Chen, Y.; Qian, C.; Sun, J. *Organometallics* **2003**, *22*, 1231.

(25) We applied for a China patent (CN 1322717) in January 2001. Basf Company promulgated a WO Patent (01/07491) in February 2001, in which two halogen-substituted 2,6-bis(imino)pyridyl iron complexes, 2,6-bis-diacetylpyridinebis(2,6-dibrom-4-methylanil)$FeCl_2$ and 2,6-bis-diacetylpyridinebis(2,6-dichloroanil)$FeCl_2$, appeared, but there was no characterization of the complexes.

(26) Britovsek, G. J. P.; Bruce, M. S.; Gibson, V. C.; Kimberley, B. S.; Maddox, P. J.; McTavish, S. J.; Redshaw, C.; Solan, G. A.; Strömberg, S.; White, A. J. P.; Williams, D. J. *J. Am. Chem. Soc.* **1999**, *121*, 8728.

(27) Qian, C.; Gao, F.; Chen, Y.; Gao, L. *Synlett.* (in press).

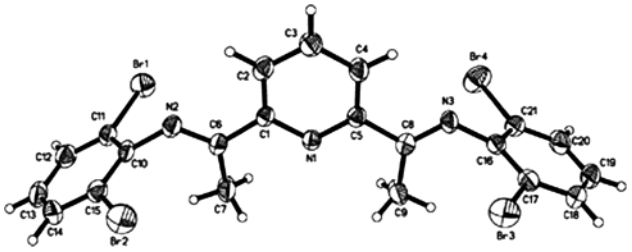

Figure 1. Molecular structure of ligand **L1**. Selected bond lengths (Å) and angles (deg): N(2)−C(6) 1.284(7), N(3)−C(8) 1.261(7); C(1)−C(6)−N(2) 116.5(6), C(5)−C(8)−N(3) 116.2(6), N(1)−C(1)−C(6) 114.6(5), N(1)−C(5)−C(8) 114.9.

acterized by elemental analysis, ^{1}H NMR, IR, and mass spectrometry. Ligand **L1** was further characterized by X-ray diffraction (Figure 1). It is observed that the ligand **L1** is in the (*E*, *E*) conformation with typical imino C═N double bonds, 1.284(7) and 1.261(7) Å. ^{1}H NMR spectra of ligands **L3**−**L6** indicate that the aryl groups bearing only a single *ortho* substituent on each aryl ring can rotate around the carbon−nitrogen bond to interconvert *syn* and *anti* isomers.[28]

The corresponding iron and cobalt complexes were synthesized by dissolving $FeCl_2 \cdot 4H_2O$ or $CoCl_2$ in tetrahydrofuran (THF) (Scheme 1), followed by addition of the appropriate ligand. The iron and cobalt complexes precipitated from the reaction solution. After washing with diethyl ether, the complexes **1**−**11** were obtained in good yield and high purity. The complexes were characterized by elemental analyses and IR spectrometry. The elemental analyses results reveal that the components of all complexes are in accord with the formula $MLCl_2$, and in some cases one solvent molecule of THF or water molecule is found in the complex. The IR spectra of the free ligands show that the C═N stretching frequencies appear in the range from 1634 to 1646 cm^{-1}. For complexes **1**−**11**, the C═N stretching vibrations shift toward lower frequencies between 1614 and 1627 cm^{-1} and are greatly reduced in intensity, which indicate the coordination interaction between the imine nitrogen atoms and the metal center. Further characterization of these complexes was difficult because of their poor solubility in organic solvents. Fortunately, single crystals of complexes **1**, **8**, **9**, **10**, and **11** suitable for X-ray diffraction analysis were obtained and characterized. The crystal structures of complexes **1**, **9**, and **10** (isomorphous with **8**) are shown in Figures 2, 3, and 4, respectively, and selected bond lengths and angles are listed in Table 1.

As shown in Figure 2, the complex **1** possesses a structure with approximate C_s symmetry about a plane containing the iron atom, the two chloro atoms, and the pyridyl nitrogen atom. One dibromophenyl ring lies almost perpendicular (81.9°) to the plane formed by the coordinated nitrogen atoms, while the other dibromophenyl ring forms a dihedral angle of 69.4° with the plane. The iron atom deviates 0.40 Å from this coordinated plane. The geometry at the iron center can be better described as distorted square pyramidal (Figure 5). The Fe−Cl(2) bond length (2.307(4) Å) is longer than that of Fe−Cl(1) (2.275(3) Å), which can be ascribed to apical elongation in the square-pyramidal complex. The two N(1)−M−Cl angles are unsymmetrical; one is 146.3(3)°, while the other is 106.6(2)°.

Table 1. Selected Bond Lengths (Å) and Angles (deg) for Complexes 1, 8, 9, and 10

	1 [M = Fe]	**8** [M = Co]	**9** [M = Fe]	**10** [M = Co]
M−N(1)	2.120(8)	2.022(5)	2.119(9)	2.04(1)
M−N(2)	2.240(9)	2.215(6)	2.189(11)	2.22(1)
M−N(3)	2.230(8)	2.217(6)	2.210(11)	2.23(1)
M−Cl(1)	2.275(3)	2.247(2)	2.265(4)	2.247(5)
M−Cl(2)	2.307(4)	2.2569(18)	2.292((4)	2.255(4)
C(6)−N(2)	1.27(1)	1.295(7)	1.250(13)	1.28(2)
C(8)−N(3)	1.29(1)	1.285(8)	1.271(17)	1.25(2)
N(1)−M−Cl(1)	146.3(3)	134.16(12)	127.8(3)	132.9(3)
N(1)−M−Cl(2)	106.6(2)	107.38(16)	113.8(3)	106.6(3)
Cl(1)−M−Cl(2)	107.0(1)	118.45(7)	118.27(16)	120.5(2)
N(1)−M−N(2)	71.6(3)	75.3(3)	73.8(4)	75.1(4)
N(1)−M−N(3)	72.3(3)	75.1(3)	73.9(5)	74.6(4)
N(2)−M−N(3)	141.1(3)	150.0(3)	147.8(4)	149.5(4)
Cl(1)−M−N(2)	95.8(2)	98.18(17)	103.3(3)	97.8(3)
Cl(1)−M−N(3)	106.2(2)	98.89(19)	96.2(3)	100.5(4)
Cl(2)−M−N(2)	105.4(2)	95.78(14)	95.8(3)	94.9(3)
Cl(2)−M−N(3)	98.4(2)	97.48(16)	97.3(3)	96.5(4)

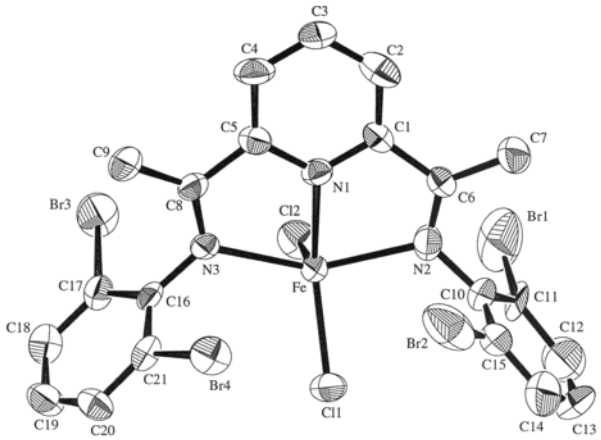

Figure 2. Molecular structure of complex **1**.

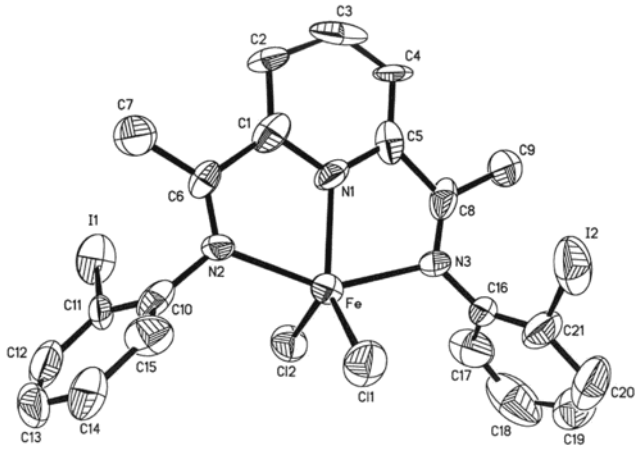

Figure 3. Molecular structure of the dominant conformation present in the crystals of **9** (one THF molecule in the lattice is not included).

The solid-state structures of the complexes with only one *ortho* substituent on the imine aryls are observed to be disordered with "up" or "down" orientation of the aryl rings. The dominant conformation of the complexes **9** (ca. 85%) displays C_2 symmetry about a plane containing the iron atom, the two chloro groups, and the pyridyl nitrogen atom. However, the dominant conformers of the complexes **8** (ca. 80%) and **10** (ca. 70%) are isomorphous (Figure 3), both having approximate C_s

(28) Gates, D. P.; Svejda, S. A.; Oñate, E.; Killian, C. M.; Johnson, L. K.; White, P. S.; Brookhart, M. *Macromolecules* **2000**, *33*, 2320.

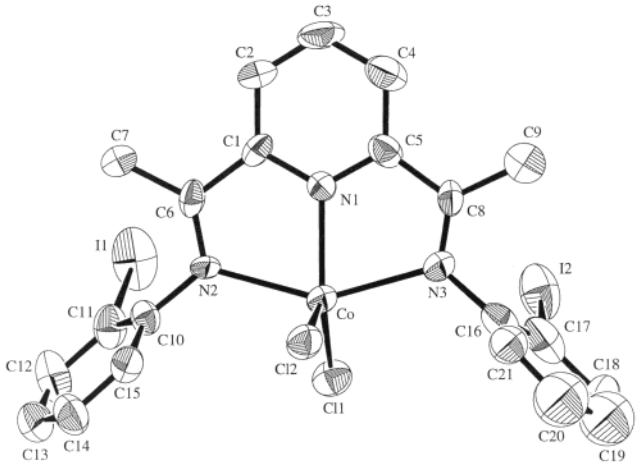

Figure 4. Molecular structure of the dominant conformation present in the crystals of **10** (that of the bromine-substituted analogue **8** is isomorphous, and one THF molecule in the lattice is not included).

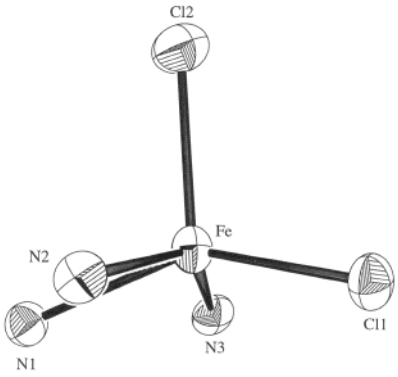

Figure 5. Coordination geometry of complex **1**.

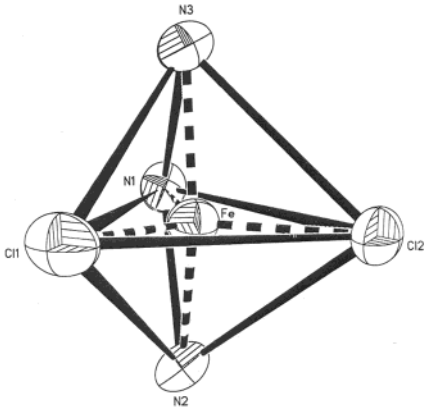

Figure 6. Coordination geometry of complex **9** (those of complexes **8** and **10** are isomorphous).

symmetry (Figure 4). The deviations of the metal ion from the plane formed by the coordinated nitrogen atoms in **8**, **9**, and **10**, 0.006, 0.080, and 0.006 Å, respectively, are much less than that in **1**. As shown in Figure 6, the geometry at the metal center in these three complexes can be described as distorted trigonal bipyramidal with the equatorial plane formed by the pyridyl nitrogen atom, the two chloro ligands, and the two axial Fe−N bonds (Figure 6). The metal ions lie only 0.013, 0.041, and 0.025 Å out of the equatorial plane in **8**, **9**, and **10**, respectively. The Cl(1)−M−Cl(2) angles are very similar for these three complexes (118.45(7)° in **8**,

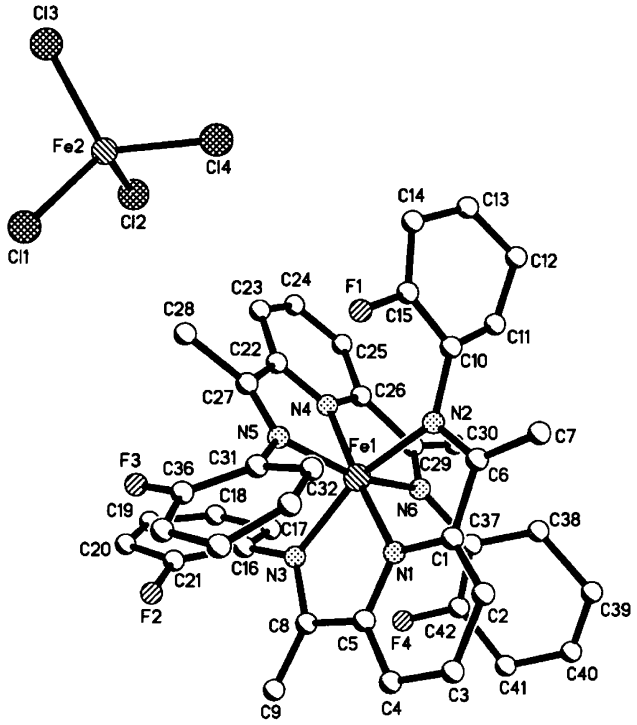

Figure 7. Molecular structure of complex **11** (one water molecule in the lattice is not included). Selected bond lengths (Å) and angles (deg): Fe(1)−N(1) 1.863(8), Fe(1)−N(2) 1.968(7), Fe(1)−N(3) 1.995(7), Fe(1)−N(4) 1.844(8), Fe(1)−N(5) 1.952(6), Fe(1)−N(6) 1.979(7), Fe(2)−Cl(1) 2.295(3), Fe(2)−Cl(2) 2.302(3), Fe(2)−Cl(3) 2.303(4), Fe(2)−Cl(4) 2.313(3); N(1)−Fe(1)−N(2) 79.9(3), N(1)−Fe(1)−N(3) 81.6(3), N(2)−Fe(1)−N(3) 161.5(4), N(4)−Fe(1)−N(5) 78.9(3), N(4)−Fe(1)−N(6) 79.6(3), N(5)−Fe(1)−N(6) 158.4(4), N(4)−Fe(1)−N(1) 176.8(2).

118.27(16)° in **9**, 120.5(2)° in **10**) and much larger than the value of 107.0(1)° for complex **1**. The N(1)−M−Cl angles of complex **9** (127.8(3)° and 113.8(3)°) are different from those in complexes **8** (134.16(12)° and 107.38(16)°) and **10** (132.9(3)° and 106.6(3)°). It is worth noting that the N(1)−M−Cl angle on the same side as the halide substituents (134.16(12)° in **8** and 132.9(3)° in **10**) is much larger than the other N(1)−M−Cl angle (107.38(16)° in **8** and 106.6(3)° in **10**).

The X-ray diffraction analysis indicates that complex **11** exists as an ion pair comprised of $[FeL_2]^{2+}$ and $[FeCl_4]^{2-}$ (Figure 7). In the cation, the iron atom is coordinated by six nitrogen atoms from two ligands, and its coordination geometry at the iron center of $[FeL_2]^{2+}$ can be described as distorted octahedron. The Fe−N(imino) bonds and Fe−N(pyridyl) bonds are shorter than those in the complexes **1**, **9**, and other reported five-coordinate iron complexes by 0.2−0.3 Å[26,29] and comparable to those in the six-coordinate iron complexes with a similar type of ligand.[30] The geometry at the iron center of $[FeCl_4]^{2-}$ can be described as a distorted tetrahedron with Fe−Cl distances of 2.295(3)−2.313(3) Å and Cl−Fe−Cl angles of 101.21(8)−115.82(15)°. There is one molecule of water in the lattice, which is not coordinated with the metal ion.

(29) Britovsek, G. J. P.; Mastroianni, S.; Solan, G. A.; Baugh, S. P. D.; Redshaw, C.; Gibson, V. C.; White, A. J. P.; Williams, D. J.; Elsegood, M. R. J. *Chem. Eur. J.* **2000**, *6*, 2221.
(30) Scheer, C.; Chautemps, P.; Gautier-Luneau, I.; Pierre, J.; Serratrice, G. *Polyhedron* **1996**, *15*, 219.

Table 2. Ethylene Polymerization Results from Complexes 1−4 and 12/MMAO[a]

run	complex	temp (°C)	Al/M (mol/mol)	yield (g)	activity (10^6g/mol of cat·h)	M_w	M_n	M_w/M_n	mp (°C)
1	**1**	0	1250	3.44	8.6	101 000	1860	54.3	128
2	**1**	40	1250	2.73	6.8	52 300	1570	33.3	
3	**2**	0	1250	0.25	0.6	12 200	3580	3.41	129
4	**3**	0	1250	5.13	12.8	13 300	2570	5.18	128
5	**4**	0	1250	0.47	1.2	370	320	1.15	
6	**1**	0	2500	4.87	12.2	65 100	1350	48.2	
7	**12**[b]	0	2500	2.16	5.4	144 000	1380	104.3	
8	**1**[c]	15	1500	28.8	72.0	377 000	14300	26.4	133
9	**3**[c]	15	1500	29.2	73.0	27 700	7650	3.62	132

[a] Toluene solvent 50 mL, 1 atm of ethylene, reaction time 0.5 h, cat. 0.8 μmol. [b] Precatalyst 2,6-bis-diacetylpyridinebis(2,6-diisopropylanil)$FeCl_2$ (**12**) was prepared according to the literature.[20] [c] Toluene solvent 500 mL, 6 atm of ethylene, triisobutylaluminum scavenger, reaction time 0.5 h, cat. 0.8 μmol.

Table 3. Results of Oligomerization of Ethylene with Complexes 5−11 and 13/MMAO

run	complex (μmol)	toluene (mL)	Al/M (mol/mol)	temp (°C)	press. (atm)	time (min)	yield (g)	activity (10^6g/mol of cat·h)	α	linear α-olefin (%)
1	**13**[a] (0.8)	50	1250	0	1	30	0.32	0.08	0.70	>91
2	**13**[a] (1)	150	2000	60	10	60	38.4	38.4	0.42	>98
3	**5** (0.8)	50	1250	0	1	30	2.4	6.0	0.69	>94
4	**5** (1)	150	2000	40	10	60	25.3	25.3	0.70	>98
5	**5** (1)	150	2000	60	10	60	51.9	51.9	0.59	>98
6	**6** (2)	150	1500	60	10	60		inactive		
7	**7** (0.8)	50	1250	0	1	30	1.7	4.3	0.83	>94
8	**7** (2)	150	1500	60	10	60	58.1	29.5	0.63	>98
9	**8** (2)	150	1500	60	10	60		inactive		
10	**9** (2)	50	1250	0	1	30	trace			
11	**9** (2)	150	1500	60	10	60	18.5	9.3	0.67	>98
12	**10** (2)	150	1500	60	10	60		inactive		
13	**11** (1)	150	1500	60	10	25		inactive		
14	**11** (1)	150	1500	60	10	40		inactive		

[a] 2,6-Bis-diacetylpyridinebis(2,6-difluoroanil)$FeCl_2$ (**13**).

2.2. Ethylene Polymerization and Oligomerization. Ethylene polymerization and oligomerization catalyzed by these iron and cobalt coordination complexes using modified methylaluminoxane (MMAO) as cocatalyst have been systematically investigated. The results are listed in Tables 2 and 3.

2.2.1. Substituent Effects of Aryl Ring on Catalyst Activity and Product Properties. Ligand environment has a great influence on the catalyst behaviors, such as activity and product properties. The iron complexes bearing a 2,6-bis(imino)pyridyl ligand with bromo (**1**) and chloro (**3**) substituents at both *ortho* positions of the aryl rings, respectively, activated with MMAO produce high molar mass polyethylene. The molar mass is strictly substituent dependent; the molar mass M_w decreases from 101 000 generated by bromo-substituted iron complex **1** to 13 300 by the chloro-substituted iron complex **3** under the conditions of 0 °C, 1 atm ethylene pressure, and 1250 Al/Fe molar ratio. Complex **3** shows higher activity than that of **1**: 12.8×10^6 g/mol of cat·h for **3** vs 8.6×10^6 g/mol of cat·h for **1**. Complex **1** is more active in ethylene polymerization (12.2×10^6 g/mol of cat·h) than the corresponding isopropyl-substituted iron complex **12**[20,22,26] (5.4×10^6 g/mol of cat·h) reported by Brookhart and Gibson under identical conditions of 0 °C, 1 atm, and Al/Fe molar ratio 2500. The electron-withdrawing nature of chloro and bromo substituents, which results in a more electrophilic iron center in the complexes, may increase the corresponding activity in the ethylene polymerization. The semiempirical calculation[31] indicates the atomic (Mulliken) charges on the irons in the complexes with isopropyl or methyl substituents in both *ortho* aryl positions are very close, −0.2859 and −0.2854, respectively. The charge on the iron center in the chloro-substituted complex **3** (−0.2354) is more positive than that in the bromo-substituted complex **1** (−0.2502), and compared with the complexes with alkyl substitutes, the halogen-substituted complexes **3** and **1** have relatively more positive iron centers. When the *ortho* positions of the aryl rings of the ligand are filled by fluoro groups, the corresponding complex **13** generates oligomer instead of polymer (Table 3, runs 1 and 2).[24] The small size and strong electron-withdrawing nature of the fluoro group are responsible for the small α value. The atomic (Mulliken) charge on the iron in complex **13** with fluoro substiuents is −0.1862, which is comparable to that in the complex with $-CF_3$ substituents, −0.1813.

The cobalt complexes show the same trends as iron complexes, with higher activity and lower molar mass product for chloro-subsituted complexes than those of bromo-subsituted complexes, although their activities are much lower than those of the iron analogues.

Compared with **1** and **3**, in which both *ortho* positions of the aryl rings are substituted by bromo and chloro groups, respectively, the iron complexes with only one *ortho* substituent on the aryl rings, **5** and **7**, show lower activity and provide much lower molar mass products in the ethylene polymerization. The distribution of oligomers obtained by **5** and **7** follows Schulz−Flory

(31) Semiempirical PM3 calculations were carried out on complexes **8**, **10**, **12**, **21**, a complex with $-CH_3$ substituents in both *ortho* aryl positions, and a complex with $-CF_3$ substituents in both *ortho* aryl positions. Their geometries were fully optimized for the quintet state of each compound,[26,29] using the standard procedure with conventional gradient techniques. The atomic (Mulliken) charge on the iron atom was thus obtained.

rules, which can be characterized by a constant α, where α represents the probability of chain propagation [α = rate of propagation/(rate of propagation + rate of chain transfer) = mol of C_{n+2}/mol of C_n].[32−36] The α value can be determined by the molar ratio of C_{12} and C_{14} fractions. Under the conditions of 0 °C, 1 atm, and Al/Fe molar ratio of 1250, the activities of mono *ortho*-substituted complexes **5** and **7** (6.0×10^6 and 4.3×10^6 g/mol of cat·h) are about half of the corresponding double *ortho*-substituted complexes **3** (12.8×10^6 g/mol of cat·h) and **1** (8.6×10^6 g/mol of cat·h). In addition, the bromo-substituted complex **7** exhibits lower activity than the chloro-substituted complex **5**, but the molar mass of products produced by **7** are higher than those produced by **5**. Similar trends are observed for these complexes under other conditions, such as at 60 °C and 10 atm of ethylene pressure. Changing the substituents to iodo groups, complex **9**, results in a great decrease in activity. The activity of **9** is too low to yield meaningful product at 1 atm. When the ethylene pressure was raised to 10 atm, the activity increases to 9.3×10^6 g/mol of cat·h with the oligomer's α value of 0.67, which is higher than the α values of oligomers generated by **5** (0.59) and **7** (0.63) under similar conditions. GC−MS and GC analyses indicate that complexes **5**, **7**, and **9** produced linear α-olefins with a selectivity higher than 98% at 10 atm. Complex **11**, containing the ligand with only one fluoro group on the *ortho* aryl position, is found to be inactive for ethylene oligomerization (Table 3, runs 13, 14), which is probably due to the ion-pair structure. The iron complex bearing a bis(imino)pyridyl ligand without substituents on either of the *ortho* aryl positions is also prepared for comparison. It is inactive for ethylene oligomerization, which may also be associated with the ion-pair structure of the complex.[37−39]

2.2.2. Metal Center Effects on the Catalyst Activity and Product Properties. Similar to the observation in metal coordinative complexes with alkyl substituents on the *ortho* positions of the aryl rings of the ligands, the cobalt complexes show much lower activity and yield product with lower molar mass than their iron analogues. The activities of cobalt complexes **2** and **4** are approximately an order of magnitude less active than those of their iron analogues **1** and **3**. The molar masses M_w of polyethylene generated from **2** and **4** dropped to 12 200 and 370, respectively, compared to those for the corresponding iron anologues **1** (101 000) and **3** (13 300). The cobalt complexes **6**, **8**, and **10** all gave unsuccessful results in ethylene polymerization.

NMR analyses reveal that the iron and cobalt complexes **1**−**4** generated highly linear polymers. The end groups of polyethylene yielded from iron complexes are mainly saturated end groups, whereas the cobalt complexes generate polymers with unsaturated chain ends. This is probably because of different chain transfer mechanisms during the reaction. For the iron complexes, matured polymer chains formed in the polymerization mainly transfer to aluminum complexes; subsequent quenches with ethanol generate saturated polyethylene. For the cobalt complexes, β-H elimination is the major factor in chain transfer, which gives unsaturated polymer chain ends. The linearity was also reflected in the thermal properties of the polymers. The melting points are found to be in the range 128−133 °C for complexes **1**−**3** (Table 2, runs 1, 3, 4, 8, 9).

Table 4. Effects of Al/Fe Molar Ratio on Ethylene Polymerization with Complex 1[a]

run	Al/Fe (mol/mol)	yield (g)	activity (10^6g/mol of cat·h)	M_w	M_n	M_w/M_n
1	250	1.27	3.2	184 000	15 600	11.8
2	1250	3.44	8.6	101 000	1860	54.3
3	2500	4.87	12.2	65 100	1350	48.2
4	5000	4.02	10.1	19 400	840	23.0

[a] Toluene solvent 50 mL, 1 atm of ethylene, 0 °C, reaction time 0.5 h, cat. 0.8 μmol.

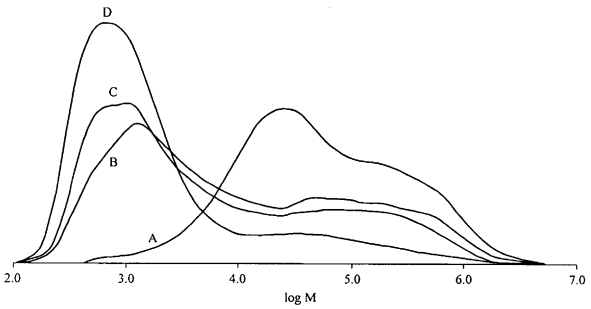

Figure 8. Effect of Al/Fe molar ratio on the molar masses of polymers produced with complex **1**. A: Al/Fe = 250; B: Al/Fe = 1250; C: Al/Fe = 2500; D: Al/Fe = 5000.

2.2.3. Effects of Reaction Conditions on the Catalyst Activity and Product Properties. Effects of Al/Fe Molar Ratio. It has been found that Al/Fe molar ratio has a significant effect on the ethylene polymerization behavior for alkyl-substituted iron complexes.[20,26] The experiments were carried out to elucidate effects of Al/Fe molar ratio on ethylene polymerization using halogen-substituted iron complexes as precatalysts activated with MMAO. Complex **1** was selected as an example, and the Al/Fe values were systematically varied from 250 to 5000. The results are summarized in Table 4, and the curvatures of GPC analyses are shown in Figure 8.

The molar mass distributions of the samples obtained at different Al/Fe molar ratios are bimodal. Raising the Al/Fe molar ratio results in an increase of the lower molar mass fraction. For example, the lower molar mass fraction of about 50% of the sample obtained at an Al/Fe molar ratio of 250 increases to 60% at an Al/Fe of 1250 and 75% at an Al/Fe of 2500. Raising the Al/Fe molar ratio to 5000, the lower molar mass fraction is most prominent, accounting for over 90% of the sample. It is also found that the average polymer molar mass of the lower molar mass fraction decreases with increasing Al/Fe molar ratio. These evidenced that the molecular chains transferred to the aluminum complexes during the polymerization and the higher Al/Fe value increase the rate of chain transfer to the Al complex. When the polymerization is quenched, it gives the saturated polymer product. This is in good agreement with polymer analysis results disscussed in section 2.2.2.

(32) Svejda, S. A.; Brookhart, M. *Organometallics* **1999**, *18*, 65.
(33) Schulz, G. V. Z. *Phys. Chem., Abt. B.* **1935**, *30*, 379.
(34) Schulz, G. V. Z. *Phys. Chem., Abt. B.* **1939**, *43*, 25.
(35) Flory, P. J. *J. Am. Chem. Soc.* **1940**, *62*, 1561.
(36) Henrici-Olivé, G.; Olivé, S. *Adv. Polym. Sci.* **1974**, *15*, 1.
(37) Curry, J. D.; Robinson, M. A.; Busch, D. H. *Inorg. Chem.* **1967**, *6*, 1570.
(38) Figgins, P. E.; Busch, D. H. *J. Am. Chem. Soc.* **1960**, *82*, 820.
(39) Lions, F.; Martin, K. V. *J. Am. Chem. Soc.* **1957**, *79*, 2733.

Table 5. Effects of Ethylene Pressure on Polymerization with Complex 2[a]

run	pressure (atm)	yield (g)	activity (10^6g/mol of cat·h)	M_w	M_n	M_w/M_n
1	4	1.00	3.33	5100	2080	2.46
2	8	1.67	5.57	5190	2090	2.49
3	12	2.07	6.90	5300	2060	2.57

[a] Toluene solvent 200 mL, Al/Co molar ratio of 1000, 25 °C, reaction time 20 min, cat. 1 μmol.

Temperature Effects on the Polymerization. It is well known that temperature has great effects on olefin polymerization, particularly on catalyst activity and polymer molar mass. For example, molar mass M_w of polymer generated by **1** drops from 101 000 at 0 °C (Table 2, run 1) to 52 300 at 40 °C (Table 2, run 2). The variation of molar mass with reaction temperature suggests an increase in the rate of chain transfer relative to the rate of propagation. In general, the reaction temperature will increase the catalyst activity in polymerization. However, for **1** the catalytic activity drops from 8.6×10^6 g/mol of cat·h to 6.8×10^6 g/mol of cat·h when the temperature increases from 0 °C (Table 2, run 1) to 40 °C (Table 2, run 2). The decrease in activity with increasing reaction temperature is mainly caused by catalyst decomposition and lower ethylene solubility at higher temperature.[26]

Ethylene Pressure Effects on the Polymerization. For iron complexes **1** and **3**, increasing the monomer pressure results in increases in activity and molar mass of polymers. At 6 atm, the activity of complex **1** increases to 72.0×10^6 g/mol of cat·h and M_w of the polyethylene obtained is up to 377 000 (Table 2 run 8). Complex **3** shows an activity of 73.0×10^6 g/mol of cat·h with the polyethylene molar mass M_w of 27 700 (Table 2 run 9). The pressure dependence of the molar mass is associated with chain propagation, aluminum chain transfer, and β-H transfer. For iron complexes, the aluminum chain transfer is an important chain transfer process. When the polymerization tests were carried out at 1 atm and Al/Fe molar ratio > 1250, aluminum chain transfer became the dominant process (see section 2.2.3). The increase of ethylene pressure results in an increase in rate of propagation and also the rate of the β-H transfer process but not the rate of aluminum chain transfer. Therefore, the rate of propagation relative to the rate of chain transfer (the rate of chain transfer = the rate of β-H transfer + the rate of aluminum chain transfer) increases with the ethylene pressure and is responsible for the higher molar mass of polymers at higher pressure.

It is different from iron complexes; there are two observations about the effects of ethylene pressure on polymerization with cobalt complexes. One is that the activity of cobalt complexes increases with ethylene pressure;[26] the other is that the activity of cobalt precatalyst does not change markedly with ethylene pressure.[1] To clarify the effects of ethylene pressure on polymerization catalyzed by halogen-substituted cobalt complexes, the experiments were carried out using cobalt complex **2** as precatalyst in the ethylene polymerization. Results with different ethylene pressure from 4 to 12 atm are listed in Table 5. The results show that the activity of ethylene polymerization catalyzed by cobalt complex **2** increases with increasing ethylene pressure, while the molar mass and molar mass distribution of polymers remain essentially invariant. These results suggest that both chain propagation and chain transfer increase equally with ethylene pressure. The different effects of ethylene pressure on the molar mass of polymers observed using iron complex **1** and cobalt complex **2** as precatalysts are due to the different chain transfer mechanisms during the reaction. For the iron complex, the chain transfer to aluminum is the main chain transfer process, at least at lower pressure and higher Al/Fe molar ratio. But for the cobalt complex, the β-H transfer to the monomer is the major chain transfer process. The different chain transfer mechanism is also reflected in the polymer structure: the end groups of the polymers generated from iron complexes are mainly saturated end groups, whereas for polymers generated from the cobalt complexes, the ratio of vinyl end groups to methyl groups is approximately 1:1.

3. Summary

Six new halogen-substituted 2,6-bis(imino)pyridyl ligands have been synthesized. Reactions of these halogen-substituted 2,6-bis(imino)pyridyl ligands with $MCl_2 \cdot nH_2O$ (M = Fe, n = 4; M = Co, n = 0) provided two types of complexes: five-coordinate complex and ion-pair complex, which is dependent on the halogen substitutents. On treatment with MMAO, all the five-coordinate iron complexes are very active for ethylene polymerization and oligomerization, while the ion-pair complex is inactive. The catalyst productivity and product properties are strictly substituent dependent. The molar mass of the product can be easily changed from high molar mass polymers to very low molar mass oligomers by using different halogen atoms as substituents.

4. Experimental Section

4.1. General Procedures. All manipulations of air- and/or moisture-sensitive compounds were performed under an atmosphere of argon using standard Schlenk techniques. ^{1}H NMR and ^{13}C NMR were recorded on Bruker Am-300 or Varian XL-300 MHz spectrometers. Mass spectra were carried out with a HP5989A spectrometer. IR spectra were recorded using Perkin-Elmer 983 or Nicolet AV-360 spectrometers. Elemental analyses were performed by the Analytical Laboratory of the Shanghai Institute of Organic Chemistry. Oligomer products were analyzed by Varian CP-3800 GC and Finnigan MD-800 GC−MS. The Varian CP-3800 GC was equipped with an SPB-5 capillary column (30 m × 0.32 mm) and a flame ionization detector. The analytic conditions used were as follows: injector and detector temperature, 280 °C; oven temperature program, 40 °C/6 min, 10 °C/min ramp, 250 °C/15 min. C_6 olefin isomer was used in determining the percentage of linear α-olefins. ^{1}H NMR and ^{13}C NMR spectra of polyethylene were taken in 1,2-dichlorobenzene-d_4 at 100 or 135 °C. High-temperature gel permeation chromatography (GPC) was performed on PL-GPC 220 in 1,2,4-trichlorobenzene at 135 °C using polystyrene calibration. Melting temperatures of preheated samples were determined by differential scanning calorimetry (DSC) with a Perkin-Elmer pryris at a heating rate of 10 °C/min. 2,6-Diacetylpyridine[40] and 2,6-bis-diacetylpyridine bis(2,6-diisopropylanil)$FeCl_2$ (**12**)[20] were prepared according to published procedures. 2-Iodoaniline was purchased from Acros and purified by recrystallization from petroleum ether.

(40) Alyes, E. C.; Merrel, P. H. *Synth. React. Inorg. Metal-Org. Chem.* **1974**, *4*, 53510.

Other anilines were purchased from TCL, Acros Organics, or Aldrich Chemical Co. and used as received. Silica−alumina catalyst support (grade 135) was purchased from Aldrich Chemical Co. Modified methylaluminoxane (MMAO) was purchased from Akzo Nobel. Tetrahydrofuran was degassed to remove oxygen prior to use. Toluene used as solvent in polymerization or oligomerization was distilled under argon over sodium−benzophenone.

4.2. Synthesis of Ligands. 2,6-Diacetylpyridinebis(2,6-dibromoanil) (L1). A solution of 2,6-dibromoaniline (1.23 g, 5.0 mmol), 2,6-diacetylpyridine (0.41 g, 2.5 mmol), and *p*-toluenesulfonic acid (0.020 g) in toluene (100 mL) was refluxed for 24 h, with azeotropic removal of water using a Dean−Stark trap. The mixture was cooled to room temperature, and the solvent was removed under reduced pressure. The crude product was dissolved in Et_2O (100 mL), and the organic layer was washed twice with water (50 mL) and once with saturated NaCl solution (50 mL) and dried over $MgSO_4$. The solvent was removed under reduced pressure, and the crude product was recrystallized from MeOH to give the desired product in 35% yield. ^{1}H NMR (300 MHz, $CDCl_3$): δ 8.55 (d, 2H, J = 7.8 Hz, Py−H_m); 7.97 (t, 1H, J = 7.8 Hz, Py−H_p); 7.58 (d, 4H, J = 8.0 Hz, Ar−H); 6.86 (t, 2H, J = 8.0 Hz, Ar−H); 2.36 (s, 6H, N=CMe). IR (KBr): 1638($\nu_{C=N}$), 1565, 1546, 1450, 1426, 1366, 1323, 1304, 1259, 1222, 1198, 1143, 1123, 1076, 969, 881, 822, 824, 762, 769, 652 cm^{-1}. EI-MS: m/z 625 [M$^+$]. Anal. ($C_{21}H_{15}N_3Br_4$) Calcd: C, 40.06; H, 2.38; N, 6.68. Found: C, 40.47; H, 2.73; N, 6.37.

2,6-Bis-diacetylpyridinebis(2,6-dichloroanil) (L2). A solution of 2,6-dichloroaniline (0.79 g, 5.0 mmol), 2,6-diacetylpyridine (0.41 g, 2.5 mmol), and *p*-toluenesulfonic acid (0.020 g) as well as 4 Å molecular sieves (0.5 g) in toluene (100 mL) was refluxed for 24 h, with azeotropic removal of water using a Dean−Stark trap. The mixture was cooled to room temperature, and the solvent was removed under reduced pressure. Workup as above yielded the desired product in 40% yield. ^{1}H NMR (300 MHz, $CDCl_3$): δ 8.52 (d, 2H, J = 7.8 Hz, Py−H_m); 7.95 (t, 1H, J = 7.8 Hz, Py−H_p); 7.35 (d, 4H, J = 8.0 Hz, Ar−H); 7.01 (t, 2H, J = 8.0 Hz, Ar−H); 2.36 (s, 6H, N=CMe). IR (KBr): 1646 ($\nu_{C=N}$), 1576, 1555, 1449, 1432, 1362, 1318, 1301, 1272, 1226, 1151, 1120, 1096, 997, 958, 917, 827, 789, 777, 752, 653 cm^{-1}. EI-MS: m/z 449 [M$^+$]. Anal. ($C_{21}H_{15}N_3Cl_4$) Calcd: C, 55.88; H, 3.33; N, 9.31. Found: C, 55.80; H, 3.47; N, 9.15.

2,6-Diactylpyridinebis(2-fluoroanil) (L3). A solution of 2,6-diacetylpyridine (0.41 g, 2.5 mmol), 2-fluoroaniline (0.77 g, 6 mmol), silica−alumina catalyst support (0.2 g) and molecular sieves 4 Å (1 g) in toluene (8 mL) was stirred at 30−40 °C for 24 h. The reaction mixture was filtered, and the molecular sieve was washed with toluene several times. The toluene of the combined filtrates was removed in vacuo. Anhydrous methanol (5 mL) was added to the residue. **L3** was obtained as a yellow powder in 56% yield. ^{1}H NMR (300 MHz, $CDCl_3$): δ 8.39 (d, 2H, J = 8.0 Hz, Py−H_m); 7.90 (t, 1H, J = 7.9 Hz, Py−H_p); 7.19−7.10 (m, 6H, Ar−H); 7.08−6.91 (m, 2H, Ar−H); 2.42 (s, 6H, N=CMe). IR (KBr): 1634($\nu_{C=N}$), 1601, 1575, 1482, 1364, 1236, 1194, 1123, 1102, 1079, 1031, 844, 825, 780, 760, 744 cm^{-1}. EI-MS: m/z 349 [M$^+$]. Anal. ($C_{21}H_{17}N_3F_2$) Calcd: C, 72.19; H, 4.90; N, 12.03. Found: C, 71.88; H, 4.96; N, 11.99.

2,6-Diactylpyridinebis(2-chloroanil) (L4). Using a procedure analogous to that used for the synthesis of **L3**, **L4** was obtained as a yellow powder in 65% yield. ^{1}H NMR (300 MHz, $CDCl_3$): δ 8.44 (d, 2H, J = 8.0 Hz, Py−H_m); 7.94 (t, 1H, J = 7.8 Hz, Py−H_p); 7.43 (dd, 2H, J = 8.0 Hz, Ar−H); 7.28 (pseudo t, 2H, J = 7.7 Hz, Ar−H); 7.07 (pseudo t, 2H, J = 7.8 Hz, Ar−H); 6.86 (dd, 2H, J = 7.9 Hz, Ar−H); 2.38 (s, 6H, N=CMe). IR (KBr): 1635 ($\nu_{C=N}$), 1582, 1465, 1436, 1362, 1252, 1222, 1120, 1054, 1032, 816, 772, 756, 743, 735, 687 cm^{-1}. EI-MS: m/z 381 [M$^+$]. Anal. ($C_{21}H_{17}N_3Cl_2$) Calcd: C, 65.97; H, 4.48; N, 10.99. Found: C, 65.44; H, 4.69; N, 10.88.

2,6-Diactylpyridinebis(2-bromoanil) (L5). Using a procedure analogous to that used for the synthesis of **L3**, **L5** was obtained as a yellow powder in 75% yield. ^{1}H NMR (300 MHz, $CDCl_3$): δ 8.47 (d, 2H, J = 7.7 Hz, Py−H_m); 7.94 (t, 1H, J = 7.7 Hz, Py−H_p); 7.62 (dd, 2H, J = 8.0 Hz, Ar−H); 7.34 (pseudo t, 2H, J = 7.6 Hz, Ar−H); 7.01 (pseudo t, 2H, J = 7.6 Hz, Ar−H); 6.85 (dd, 2H, J = 7.9 Hz, Ar−H); 2.38 (s, 6H, N=CMe). IR (KBr): 1634 ($\nu_{C=N}$), 1574, 1430, 1360, 1252, 1220, 1025, 816, 770, 754, 734 cm^{-1}. EI-MS: m/z 469 [M$^+$]. Anal. ($C_{21}H_{17}N_3Br_2$) Calcd: C, 53.53; H, 3.64; N, 8.92. Found: C, 53.66; H, 3.65; N, 8.88.

2,6-Diactylpyridinebis(2-iodoanil) (L6). Using a procedure analogous to that used for the synthesis of **L3**, after 48 h, the reaction mixture was filtered and the molecular sieve was washed with toluene several times. The toluene of the filtrate was removed in vacuo. Petroleum ether (10 mL) was added to the residue. A yellow solid formed, which was filtered off to afford **L6** in 64% yield. ^{1}H NMR (300 MHz, $CDCl_3$): δ 8.52 (d, 2H, J = 7.5 Hz, Py−H_m); 7.96 (t, 1H, J = 8.0 Hz, Py−H_p); 7.90 (dd, 2H, J = 7.8 Hz, Ar−H); 7.37 (pseudo t, 2H, J = 7.5 Hz, Ar−H); 6.85 (pseudo t, 2H, J = 7.6 Hz, Ar−H); 6.80 (dd, 2H, J = 7.8 Hz, Ar−H); 2.37 (s, 6H, N=CMe). IR (KBr): 1645 ($\nu_{C=N}$), 1568, 1457, 1431, 1364, 1252, 1218, 1116, 1017, 830, 813, 772, 656 cm^{-1}. EI MS: m/z 565 [M$^+$]. Anal. ($C_{21}H_{17}N_3I_2$) Calcd: C, 44.63; H, 3.03; N, 7.43. Found: C, 44.95; H, 3.06; N, 7.30.

4.3. Synthesis of Complexes. 2,6-Bis-diacetylpyridinebis(2,6-dibromoanil)$FeCl_2$ (1). Ligand **L1** (191 mg, 0.30 mmol) was added to a solution of $FeCl_2{\cdot}4H_2O$ (56 mg, 0.28 mmol) in THF (12 mL) at room temperature with rapid stirring. The solution turned to deep blue immediately. The dark blue product precipitated from the solution after several minutes. After being stirred at room temperature for 12 h, the reaction volume was reduced to about 6 mL. The reaction mixture was allowed to stand at room temperature for several hours, then the supernatant liquid was removed. The product was washed with 4 × 5 mL of Et_2O and dried in vacuo. The desired product (0.170 mg) was obtained as a blue powder in 80% yield. IR (KBr): 1614($\nu_{C=N}$), 1587, 1555, 1429, 1371, 1265, 817, 771, 730 cm^{-1}. Anal. ($C_{21}H_{15}N_3Br_4FeCl_2$) Calcd: C, 33.37; H, 2.00; N, 5.56. Found: C, 33.67; H, 2.14; N, 5.47.

2,6-Bis-diacetylpyridinebis(2,6-dibromoanil)$CoCl_2$ (2). This golden brown complex was prepared as above in 80% yield, using ligand **L1** (397 mg, 0.63 mmol) and $CoCl_2$ (82 mg,0.63 mmol). IR (KBr): 1617($\nu_{C=N}$), 1584, 1551, 1428, 1368, 1319, 1267, 1234, 1194, 1022, 824, 816, 769, 726 cm^{-1}. Anal. ($C_{21}H_{15}N_3Br_4CoCl_2$) Calcd: C, 33.25; H, 1.98; N, 5.54. Found: C, 33.18; H, 2.17; N, 5.58.

2,6-Bis-diacetylpyridinebis(2,6-dichloroanil)$FeCl_2$ (3). This blue complex was prepared as above in 85% yield, using ligand **L2** (285 mg, 0.63 mmol) and $FeCl_2{\cdot}4H_2O$ (125 mg, 0.63 mmol). IR (KBr): 1623($\nu_{C=N}$), 1583, 1558, 1435, 1373, 1267, 1235, 1099, 1023, 819, 793, 773 cm^{-1}. Anal. ($C_{21}H_{15}N_3FeCl_6$) Calcd: C, 43.60; H, 7.27; N, 2.60. Found: C, 43.76; H, 7.31; N, 2.86.

2,6-Bis-diacetylpyridinebis(2,6-dichloroanil)$CoCl_2$ (4). This golden brown complex was prepared as above in 80% yield, using ligand **L2** (285 mg, 0.63 mmol) and $CoCl_2$ (82 mg,0.63 mmol). IR (KBr): 1626($\nu_{C=N}$), 1583, 1557, 1436, 1373, 1268, 1236, 1096, 1025, 820, 793, 773 cm^{-1}. Anal. ($C_{21}H_{15}N_3CoCl_6$) Calcd: C, 43.45; H, 2.59; N, 7.24. Found: C, 43.13; H, 2.71; N, 7.21.

2,6-Bis-diacetylpyridinebis(2-chloroanil)$FeCl_2$ (5). This blue complex was prepared as above in 75% yield, using ligand **L4** (172 mg, 0.45 mmol) and $FeCl_2{\cdot}4H_2O$ (80 mg, 0.40 mmol). IR (KBr): 1623 ($\nu_{C=N}$), 1587, 1470, 1440, 1373, 1262, 1228, 1060, 1033, 820, 778, 759, 745, 730, 688 cm^{-1}. Anal. ($C_{21}H_{17}N_3Cl_2FeCl_2$) Calcd: C, 49.55; H, 3.37; N, 8.25. Found: C, 49.76; H, 3.96; N, 7.59.

2,6-Bis-diacetylpyridinebis(2-chloroanil)$CoCl_2$ (6). This yellow-green complex was prepared as above in 85% yield,

Table 6. Crystallographic Data and Refinement for Ligand L1 and Complexes 1, 8, 9, 10, and 11

	L1	1	8	9	10	11
formula	$C_{21}H_{15}N_3Br_4$	$C_{21}H_{15}N_3Br_4FeCl_2$	$C_{21}H_{17}N_3Br_2$-$CoCl_2 \cdot C_4H_8O$	$C_{21}H_{17}N_3I_2$-$FeCl_2 \cdot C_4H_8O$	$C_{21}H_{17}N_3I_2$-$CoCl_2 \cdot C_4H_8O$	$C_{42}H_{34}N_6F_4$-$Fe_2Cl_4 \cdot H_2O$
fw	629.00	755.74	673.13	764.03	767.14	970.27
color	pale yellow	dark blue	yellow-green	dark blue	yellow-green	dark blue
cryst syst	triclinic	monoclinic	monoclinic	orthorhomic	monoclinic	hexagonal
space group	$P\bar{1}$ (No. 2)	$P2(1)/c$ (No. 14)	$C2/c$ (No. 15)	$P2(1)2(1)2(1)$ (No. 19)	$C2/c$ (No. 15)	$P6(1)$ (No. 169)
a, Å	7.9236(10)	12.793(6)	27.538(2)	10.990(2)	27.960(6)	11.3198(4)
b, Å	11.5210(15)	11.899(8)	12.9011(10)	15.509(3)	13.156(4)	11.3198(4)
c, Å	12.6884(16)	16.909(9)	16.6697(14)	16.821(3)	16.621(3)	62.060(4)
α, deg	90.566(2)					
β, deg	105.744(3)	99.23(4)	112.029(2)		111.73(1)	
γ, deg	79.878(2)					120.00
V, Å^3	1096.6(2)	2540(2)	5489.9(8)	2867.0(9)	5679(2)	6886.8(5)
Z	2	4	8	4	8	6
D_{calcd}, g/cm^3	1.905	1.976	1.629	1.770	1.794	1.404
F(000)	604	1448	2680	1480	2968	2964
μ(Mo Ka), mm^{-1}	7.352	7.127	3.754	2.888	2.990	0.919
θ range, deg	1.7−28.2	2.3−26.0	1.6−28.2	1.8−25.50	2.3−25.0	2.1−28.2
no. of reflns collected	6764	5494	16 646	14 874	4996	42 039
no. of unique reflns	4890	5255	6417	5339	4880	10026
no. of obsd reflns	1940 ($I > 2\sigma(I)$)	2493 ($I > 3\sigma(I)$)	1501 ($I > 2\sigma(I)$)	1829 ($I > 2\sigma(I)$)	2004 ($I > 3\sigma(I)$)	2980 ($I > 2\sigma(I)$)
no. of params	256	281	327	307	276	502
goodness of fit	0.766	1.85	0.621	0.773	1.70	0.699
final R, R_w[a]	0.063, 0.140	0.057, 0.061	0.049, 0.081	0.058, 0.130	0.061, 0.075	0.056, 0.126
$\Delta\rho_{max,min}$/e Å^{-3}	0.75, −1.31	1.27, −1.12	0.65, −0.52	0.41, −0.39	0.92, −0.75	0.54, −0.40

using ligand **L4** (57 mg, 0.15 mmol) and $CoCl_2$ (19 mg, 0.15 mmol). IR (KBr): 1627 ($\nu_{C=N}$), 1589, 1469, 1439, 1371, 1262, 1229, 1060, 1027, 819, 780, 757, 744, 729, 688 cm^{-1}. Anal. ($C_{21}H_{17}N_3Cl_2CoCl_2$) Calcd: C, 49.25; H, 3.34; N, 8.20. Found: C, 50.02; H, 3.71; N, 7.97.

2,6-Bis-diacetylpyridinebis(2-bromoanil)FeCl$_2$·THF (7). This blue complex was prepared as above in 79% yield, using ligand **L5** (414 mg, 0.88 mmol) and $FeCl_2 \cdot 4H_2O$ (161 mg, 0.81 mmol). IR (KBr): 1623 ($\nu_{C=N}$), 1587, 1467, 1375, 1268, 1229, 1028, 816, 778, 759, 743 cm^{-1}. Anal. ($C_{21}H_{17}N_3Br_2FeCl_2 \cdot$THF) Calcd: C, 44.81; H, 3.45; N, 6.27. Found: C, 43.72; H, 3.54; N, 6.27.

2,6-Bis-diacetylpyridinebis(2-bromoanil)CoCl$_2$·THF (8). This yellow-green complex was prepared as above in 85% yield, using ligand **L5** (71 mg, 0.15 mmol) and $CoCl_2$ (19 mg, 0.15 mmol). IR (KBr): 1627 ($\nu_{C=N}$), 1588, 1466, 1366, 1261, 1228, 1027, 817, 774, 759, 744 cm^{-1}. Anal. ($C_{21}H_{17}N_3Br_2CoCl_2 \cdot$THF) Calcd: C, 44.61; H, 3.74; N, 6.24. Found: C, 44.54; H, 4.05; N, 6.17.

2,6-Bis-diacetylpyridinebis(2-iodoanil)FeCl$_2$·THF (9). This dark blue complex was prepared as above in 85% yield, using ligand **L6** (72 mg, 0.13 mmol) and $FeCl_2 \cdot 4H_2O$ (24 mg, 0.12 mmol). IR (KBr): 1620 ($\nu_{C=N}$), 1586, 1457, 1432, 1370, 1263, 1225, 1017, 816, 774, 759, 738, 720 cm^{-1}. Anal. ($C_{21}H_{17}N_3I_2FeCl_2 \cdot$THF) Calcd: C, 39.30; H, 3.30; N, 5.50. Found: C, 39.07; H, 3.18; N, 5.30.

2,6-Bis-diacetylpyridinebis(2-iodoanil)CoCl$_2$·THF (10). This yellow-green complex was prepared as above in 71% yield, using ligand **L6** (36 mg, 0.064 mmol) and $CoCl_2$ (8 mg, 0.062 mmol). IR (KBr): 1625 ($\nu_{C=N}$), 1588, 1459, 1432, 1364, 1260, 1226, 1017, 816, 774, 759, 742, 724 cm^{-1}. Anal. ($C_{21}H_{17}N_3I_2$-$CoCl_2 \cdot$THF) Calcd: C, 39.14; H, 3.28; N, 5.48. Found: C, 39.40; H, 3.03; N, 5.37.

[Fe(2,6-bis-diacetylpyridinebis(2-fluoroanil))$_2$]$^{2+}$ [FeCl$_4$]$^{2+}$·H$_2$O (11). This dark blue complex was prepared as above in 84% yield, using ligand **L3** (157 mg, 0.45 mmol) and $FeCl_2 \cdot 4H_2O$ (80 mg, 0.40 mmol). IR (KBr): 3448, 1625($\nu_{C=N}$), 1584, 1529, 1487, 1401, 1374, 1320, 1246, 1104, 808, 762 cm^{-1}. ($C_{42}H_{34}N_6F_4Fe_2Cl_4 \cdot H_2O$) Calcd: C, 52.00; H, 3.73; N, 8.66. Found: C, 52.63; H, 3.46; N, 8.13.

4.4. General Procedure for Ethylene Polymerization. (**a) Normal Pressure Polymerization.** A 100 mL flame-dried Schlenk flask equipped with a stirrer bar was placed in a water bath and purged with ethylene (1atm), followed by charging with 40 mL of toluene and 1 mmol of MMAO. The required temperature was ensured by stirring the mixture for about 20 min in the water bath. A 0.8 μmol sample of precatalyst in 10 mL of toluene was injected via syringe. Polymerization time was measured from that point. After the reaction mixture was stirred under 1 atm of ethylene pressure for 0.5 h, the polymerization was stopped by injection of 2 mL of methanol. The polymer was precipitated by pouring the reaction mixture into large volume of acidified ethanol (0.5% HCl), filtered, washed with ethanol, and then dried under vacuum at 60 °C to a constant weight.

(b) High-Pressure Polymerization. A 1 L stainless steel reactor equipped with a mechanical stirrer was heated under vacuum for at least 2 h over 85 °C, allowed to cool to the required reaction temperature under ethylene atmosphere, and charged with 450 mL of toluene and 0.15 mL of Al(^{i}Bu)$_3$. The reactor was sealed and pressurized to 5 atm of ethylene pressure. Stirring for about 1 h ensured that the solution was equilibrated and the required reaction temperature was established. The ethylene pressure was then released. Then 1.2 mmol MMAO, 0.8 μmol precatalyst in toluene (10 mL), and 40 mL of toluene were added. The reactor was sealed and pressurized to 6 atm of ethylene pressure. After the reaction was carried out for 0.5 h, the pressure was released and 2 mL of methanol was immediately injected to stop the reaction. The reaction mixture was poured into a large amount of acidified ethanol (0.5% HCl) to precipitate the resulting polymer. The polymer was filtered, washed, and dried under vacuum at 60 °C to a constant weight.

4.5. General Procedure for Ethylene Oligomerization. (**a) 1 atm Oligomerization.** Similar to the procedure above for the ethylene polymerization under 1 atm pressure, the ethylene oligomerization was carried out under 1 atm of ethylene pressure at the required temperature and quenched by the injection of diluted hydrochloric acid. The organic layer was separated and dried over anhydrous Na_2SO_4. An aliquot of this solution was analyzed by GC to determine the content of oligomers.

(b) High-Pressure Oligomerization. The high pressure of ethylene oligomerization method is similar to the high-

pressure ethylene polymerization. The oligomerization was carried out in a 500 mL stainless steel reactor equipped with mechanical stirrer under required conditions. The reaction was terminated by the injection of diluted hydrochloric acid, and the oligomer was collected and worked up as described as in the oligomerization under 1 atm.

4.6. X-ray Crystallographic Studies. Data for complexes **1** and **10** were collected at 20 °C on a Rigaku AFC7R diffractometer with graphite-monochromated Mo Kα radiation ($\lambda = 0.71069$ Å). An empirical absorption correction based on azimuthal scans of several reflections was applied. The data were corrected for Lorentz−polarization effects. The structures were solved by heavy-atom Patterson methods for **1** and direct methods for **10**, and expanded using Fourier techniques. The nonhydrogen atoms were refined anisotropically by full-matrix least squares. Hydrogen atoms were included but not refined. Scattering factors were taken from ref 41. All calculations were performed using the TEXSAN crystallographic software package.[42]

Data collections for ligand **L1** and complexes **8**, **9**, and **11** were performed at 20 °C on a Bruker SMART diffractometer with graphite-monochromated Mo Kα radiation ($\lambda = 0.71073$ Å). The SMART program package was used to determine the unit-cell parameters. A SADABS absorption correction was applied, The structures were solved by direct methods and refined on F^2 by full-matrix least-squares techniques with anisotropic thermal parameters for non-hydrogen atoms. Hydrogen atoms were placed at the calculated positions and were included in the structure calculation without further refinement of the parameters. All calculations were carried out using the SHELXS-97 program. Crystal data and processing parameters for ligand **L1** and complexes **1**, **8**, **9**, **10**, and **11** are summarized in Table 6.

Acknowledgment. We are grateful to the Chinese Academy of Science and the Nature Science Foundation of China for financial support. We also thank Dr. Fuquan Song of the University of Anglia and Prof. Lixin Dai and Yong Tang of Shanghai Institute of Organic Chemistry for their helpful discussions.

Supporting Information Available: X-ray crystallographic data for structure determination of **L1**, **1**, **8**, **9**, **10**, and **11**. This material is available free of charge via the Internet at http://pubs.acs.org.

OM0302894

(41) Cromer, D. T.; Waber, J. T. *International Tables for X-ray Crystallography*; Kynoch Press: Birmingham, 1974; Vol. 4, Table 2.2A.
(42) *TEXSAN*, Crystal Structure Analysis Package; Molecular Structure Corporation: Houston, TX, 1985 and 1992.